Analysis of an AC Gas Display Panel

Abstract: The details and results for a one-dimensional numerical analysis of the gaseous discharge occurring at a single intersection of an ac gas panel are reported. A particular object of the program is the determination of the electric field magnitude as a function of both position and time, taking into account the field distortion due to the space charge. The calculations are based on the Townsend avalanche mechanism but omit the dynamic role of metastable neon atoms in a Penning gas mixture. The calculated electrical properties of the panel are compared with experimental values.

Symbols and units

· · · · · · · · · · · · · · · · · · ·	
A = Area	cm ²
C = Dielectric capacitance	F
$C_{\rm g} = \text{Gap capacitance}$	F
d = Gap width	cm
E(I) = Electric field intensity in I th box	$V \cdot cm^{-1}$
i = Total current in external circuit	Α
i_n = Current in external circuit due to	Α
motion of electrons in gas	
i_p = Current in external circuit due to	Α
motion of ions in gas	
$N_{\rm c}$ = Number of electrons leaving the	
cathode during a time interval	
N(I) = Number of electrons which pass by	
right edge of box I	
n(I) = Electron density in I th box	cm^{-3}
P = Gas pressure	Pa
p(I) = Ion density in I th box	cm^{-3}
$Q_{\rm n}$ = Charge flow in external circuit due to	C
motion of electrons	
$Q_{\rm p}$ = Charge flow in external circuit due to	C
motion of ions	
q = Magnitude of electron (ion) charge	C
R = Ambipolar electron-ion	$cm^3 \cdot s^{-1}$
recombination rate	
t = Time	S
$\Delta t = \text{Time interval}$	S
V(I) = Voltage drop within a box	V
$V_{\rm a}$ = Amplitude of applied voltage	V
$V_{\rm c}$ = Voltage across the capacitor	V
$\Delta V_{\rm c}$ = Change in capacitor voltage per firing	V
$V_{\rm g}(t) = $ Potential across gas	V .
$v_{\rm n}(I)$ = Velocity of electrons in the <i>I</i> th box	$cm \cdot s^{-1}$

$v_{\rm p}(I) = \text{Velocity of ions in the } I \text{th box}$	cm · s
x = Distance in gas gap measured from	cm
cathode	
$\Delta x = $ Length of each box	cm
γ = Secondary electron coefficient due to	

γ = Secondary electron coemicient due to ions

 $\epsilon = ext{Dielectric constant of gas} ext{ } F \cdot ext{cm}^{-1}$ $\eta(I) = ext{Electron multiplication per volt in } I ext{th} ext{ } V^{-1}$ box

 $\rho = \text{Net charge density}$ $C \cdot \text{cm}^{-3}$

Introduction

This report describes a one-dimensional numerical analysis of the electrical discharge occurring at a single intersection in an ac gas display panel. One object of the program is to determine the magnitude of the electric field as a function of both position and time, taking into account the field distortion due to the space charge.

The model is limited to a single cell, whose structure is shown schematically, with typical dimensions, in Fig. 1. The gas chamber is bounded by thin dielectric layers at each end which insulate the gas from the metal electrodes. Since the model is one-dimensional, the discharge is considered to be contained in the well-defined column shown in the figure. Such geometry produces some field fringing, and it is acknowledged that the application of Poisson's equation in one dimension reduces the accuracy of results as compared to a two-dimensional analysis.

The gas is a neon-argon Penning mixture (Ne + 0.001 Ar) under constant pressure. As shown in Fig. 2, the cell

232

is considered to be electrically equivalent to a nonlinear gaseous conductor in series with a capacitance C, formed by the series combination of the end dielectrics.

The problem is analyzed as a cyclic series of events that determine the generation of electrons and ions in the gas. To outline this sequence, consider first the ions that are driven toward the cathode by the electric field, which is created by both the applied voltage and the wall charge produced by the previous firing. Since the ion velocities are proportional to the non-uniform field, the motion toward the cathode produces a change in ion density as a function of position. A fraction γ of the ions that arrive at the cathode in a given time increment create secondary electrons, which in turn are driven by the field toward the anode. On the way to the anode, the electrons repeatedly acquire enough energy from the field to cause ionizing collisions with neon atoms. The newly liberated electrons join the parent electrons to move rapidly toward the anode and leave behind a wake of ions. This avalanche produces an exponentially increasing density of electrons and ions as a function of position. Because the field separates the oppositelycharged particles, and since the electron mobility is much higher than the ion mobility, a positive space charge is created which distorts the field. During this time, ion-electron recombinations occur which slightly reduce the ion and electron densities. The motion of ions and electrons in the gas constitutes a current that charges the series capacitor. The voltage drop across the capacitor reduces the voltage available across the gas and further modifies the internal electric field. This process continues and in a short time most of the applied voltage appears across the capacitor, the multiplication process becomes small due to the low field, and the current decays to a small value. When the polarity of the applied voltage is reversed, the charge on the capacitor again helps to produce a high field in the gas and the process is repeated.

Lay et al. [1] have reported results which solve the continuity equations with proper boundary conditions but which assume the electric field to be constant as a function of position. Their model takes into account the dynamic influence of the metastable neon atoms on Townsend's first coefficient η for a Penning gas mixture. In contrast, this paper assumes that the static values of η , measured under dc conditions, apply. Lay's paper deals with the total potential across the gas and the way the wall charge either builds up or decays for various amplitudes of erase and write pulses followed by sustain cycles. This paper is concerned with the operating characteristics after a steady state has been achieved. The numerical means used to keep track of the density of charged particles in this paper is similar to that used by Lay.

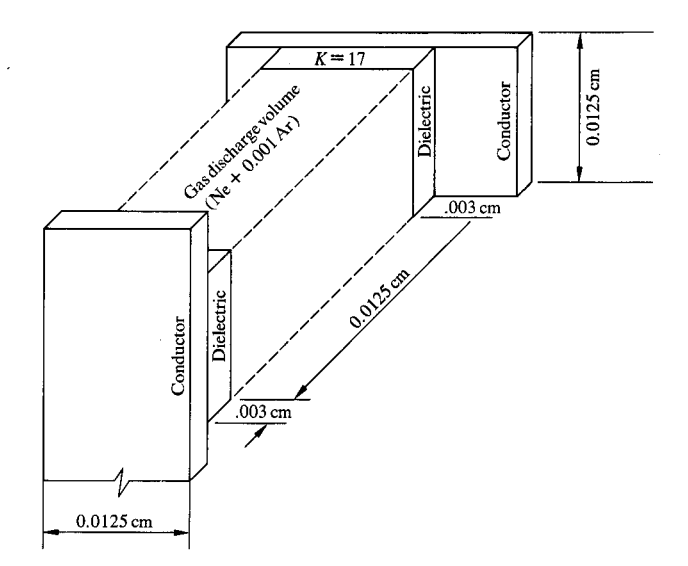


Figure 1 Structure of gas panel cell showing typical dimensions

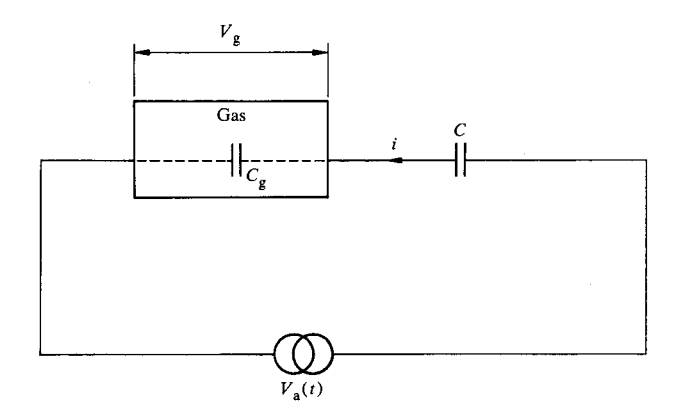


Figure 2 Equivalent electric circuit of gas panel cell.

Klein [2] has also studied this problem. His approach was to average the ion distribution over the entire gap independent of voltage and time. From this distribution the electric field was calculated and the point in space where the field became zero was considered a virtual anode. The entire voltage was then considered to be applied between the cathode and the virtual anode.

Vernon and Wang [3] have formulated a model using a sinusoidal wave drive voltage and pure neon gas. However, the boundary condition for their anode wall is not specified and the ion density they report at the anode is significantly different from the results of the current work.

Equations and assumptions

$$N(x_2) = N(x_1) \exp(\eta V). \tag{1}$$

Equation (1) is Townsend's first law, which describes how the number of electrons changes as a function of position and voltage; it assumes that $x_2 - x_1$ is small so that the electric field is essentially constant in that region. The coefficient η is a strong function of the ratio of electric field to pressure and V is the voltage drop from x_1 to x_2 .

$$N_c = \gamma P_c \tag{2}$$

Equation (2) is Townsend's second law, which simply states that the number of secondary electrons generated at the cathode is a fraction γ of the number of ions arriving at the cathode during a time interval.

Equation of continuity: $\frac{d\rho}{dt} = -dJ/dx + \text{gen. rate}$

Poisson's equation:
$$dE/dx = \rho/\epsilon$$
. (4)

Transport equations:
$$v_p = \mu_p E$$
 and $v_n = \mu_n E$. (5)

Voltage boundary condition: $V_{\sigma}(t) = V_{a}(t)$

$$-C^{-1}\int_0^t idt. \qquad (6)$$

Anode boundary condition: It is assumed that the anode collects charge as electrons arrive, but no ions or electrons are liberated into the gas from the wall.

Most of the gas mechanisms are lumped into effective values for the Townsend coefficients η and γ . The model assumes that the cell under consideration has been running in a fired mode for many cycles. The applied voltage in addition to the effect of the charge on the capacitor produced by the previous firing is adequate to maintain the cell cyclically in this mode. Since the cell is in a dynamic steady state condition, it is assumed that the published η -vs-E/P data for the gas mixture hold uniformly for all time. The values for η are those measured by Kruithof and Penning [4] and are reproduced in Table 1. It is assumed that those measurements, made at low pressures and with relatively wide gaps, apply for the higher pressure and narrower gaps used in the panel. Taking the published dc steady state values of η [4] to be time independent eliminates the need to consider in detail how the metastable neon atoms ionize the argon atoms and affect the ionization coefficient. From the point of view of this model, therefore, metastable atoms do not exist, but all of their effects are lumped into an effective η .

The coefficient γ of secondary emission at the cathode is assumed to be dominated by the arrival of ions, i.e.,

photoemission is negligible. The conclusion of a study by Lay [5] supports this assumption. This constant is treated as an adjustable parameter in the model and is chosen to produce a match between calculated and experimental values of charge transfer for one value of applied voltage, and is thereafter held fixed.

Diffusion of charge carriers is considered insignificant compared to drift velocities. However, the results showed that for a short period of time the electric field was very low in a region where a density gradient of ions existed. This could lead to an error, but the results also indicated that this error was negligible.

We assume that the neon ions quickly form Ne_2^+ at the pressure used in gas display panels. The mobility of such ions in neon is shown to be virtually independent of E[6], and its value is taken to be

$$\mu_{\rm p} = (4900/P) \,\mathrm{cm}^2/\mathrm{V} \cdot \mathrm{s}. \tag{7}$$

Anderson [7] showed that the mobility of electrons is independent of E/P in the range of 1 to 10 V/cm · Torr [(0.75 to 7.5) × 10^{-2} V/cm · Pa]. This relation is extrapolated to about 60 V/cm · Torr in the model. The mobility of electrons is about 140 times the ion mobility.

Other effects such as resonance radiation and interaction among neighboring cells are not considered in this analysis.

Method of solution

The experimental data, against which the computed solution is compared, were measured under stable conditions. To provide analogous results, the computation is run through five successive firings, each period lasting 5 μ s. The densities and charges at the end of each firing cycle become the initial conditions for the next cycle. In this way errors in the initial assumptions become unimportant. It was found that after about three cycles, the quantities are stable and cyclic. For any given set of drive inputs, only the results of the fifth cycle are considered and plotted.

Rather than attempt to code simultaneous equations with boundary conditions, the basic laws are repeatedly applied directly to each segment of space for a long series of small time intervals. The consequence of each step is accumulated so that p(x, t) and n(x, t) are established.

This process is begun by dividing the gap width into 100 equal "boxes." The procedure from this point is outlined as follows.

1. A small, uniform density of ions $(10^8/\text{cm}^3)$ is assumed initially. For typical panel dimensions, this represents about one ion per box. Since the densities of ions and electrons eventually build up to about $10^{12}/\text{cm}^3$, the initial guess serves only to get the solution started.

Table 1 Kruithof and Penning's data (Ref. 4) for (Ne⁺ 0.001 Ar) at 0°C.

E/P	η	E/P	η
0.5	0.00048	10.0	0.0322
0.6	0.00309	12.0	0.0298
0.7	0.0075	15.0	0.0279
0.8	0.0126	20.0	0.0258
0.9	0.0168	25.0	0.0243
1.0	0:0199	30.0	0.0230
1.2	0.0254	40.0	0.0215
1.5	0.0297	50.0	0.0206
2.0	0.0343	70.0	0.0193
2.5	0.0367	100.0	0.0179
3.0	0.0371	150.0	0.0160
4.0	0.0370	200.0	0.0142
5.0	0.0364	250.0	0.0127
6.0	0.0356	300.0	0.0115
8.0	0.0333	400.0	0.0090

- 2. Knowing the density of charge at each position, Poisson's equation is used to calculate the electric field intensity, and the voltage boundary condition is used to determine the constant of integration.
- 3. Since the electric field is known for each position for the time interval, it is possible to calculate the electron and ion velocity for each box using Eq. (5) and the value of η for each box. The experimental values for η -vs-E/P, shown in Table 1, were read into the computer earlier and a linear interpolation is made in the program.
- 4. A difficulty arises due to the high electron mobility. If the time increments are chosen small enough (about 10^{-12} s) to keep track of the electrons from box to box, the computer time becomes enormous. Instead, a different value of Δt is chosen for each program loop such that the ions just have time to traverse box 1 (adjacent to the cathode, where the field is maximum). This ensures that ions in other boxes move only one box or less. The details of how the electrons are handled are explained in a later section.
- 5. By keeping track of the number of charged particles that enter and leave each box, growth due to ionizing collisions, and decay due to direct recombination, a running account is kept of the ion and electron densities for each box.
- 6. From the motion of the charged particles, the current in the external circuit is calculated together with the charge transfer to the metal electrodes for each time interval.
- 7. The change of charge on the capacitor alters $V_{\rm g}$ according to Eq. (6). Using this information together with

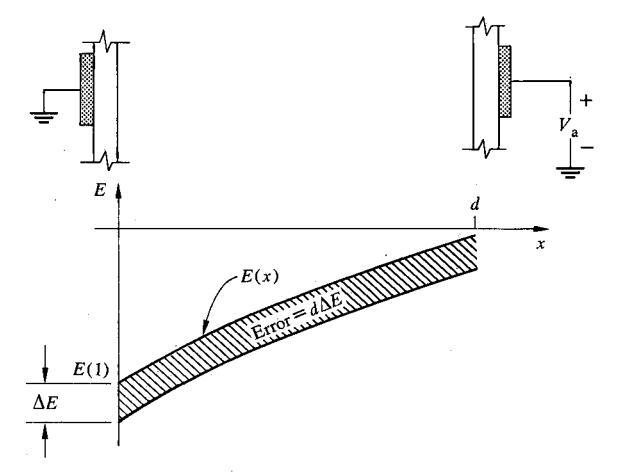


Figure 3 Variation of electric field with distance showing how the constant of integration is applied to solution of Poisson's equation.

the new charge density and voltage boundary values, the sequence of steps is repeated for the next time interval.

• Electric field

Knowing the net charge density in each box, the gradient of the electric field is given by Poisson's equation (4). This equation is integrated to give values of field at each position using the following implicit integration formula

$$E(I+1) = E(I) + \left[\frac{1}{2}(p(I) - n(I)) + \frac{1}{2}(p(I+1) - n(I+1))\right] q\Delta x/\epsilon.$$
(8)

E(1) is arbitrarily assigned the corrected value for the previous time interval and a function E(x) is generated from this point, using Eq. (8), with results as shown in Fig. 3. A constant of integration, ΔE , is added to each E(I) such that for the corrected values of electric field

$$-\sum_{I=1}^{100} E(I)\Delta x = V_{g}(t), \tag{9}$$

 $V_{\rm g}(t)$ being known from Eq. (6). Before this correction, the line integral of the field differed from $V_{\rm g}(t)$ by a small error, as shown in Fig. 3. The magnitude of ΔE is determined by setting $d\Delta E$ equal to the error. In this way a function E(x) is established which satisfies both Poisson's equation and the voltage boundary condition.

Consider now the effect on E(x) as the applied drive voltage is increased. As the cell is driven harder, the current magnitude increases, producing a greater space charge density. The increased space charge causes the gradient of the field to become steeper, while the increased current causes $V_{\rm g}$ to fall rapidly, as shown in

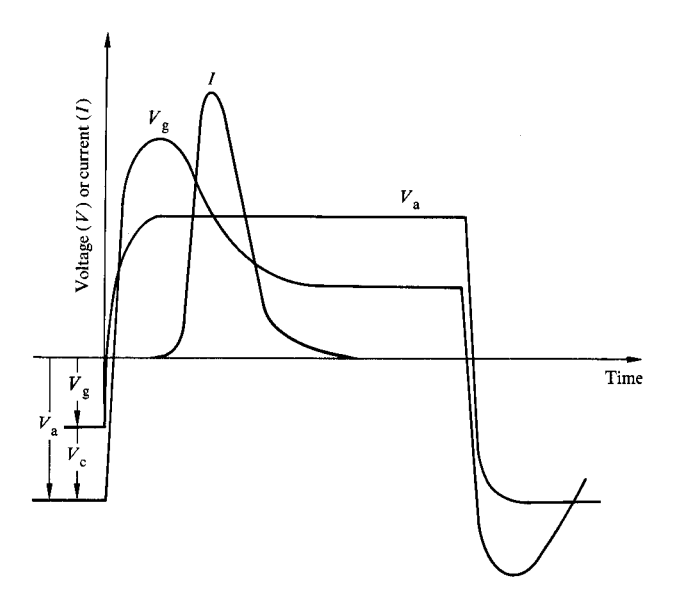
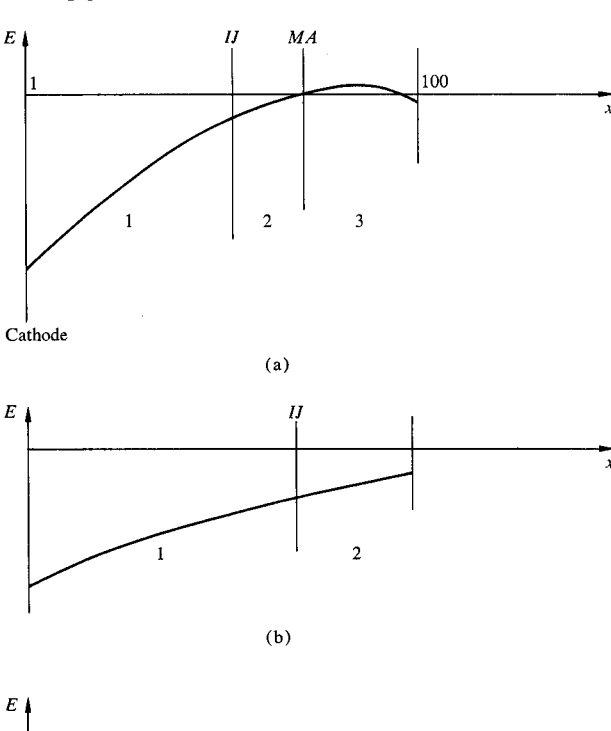
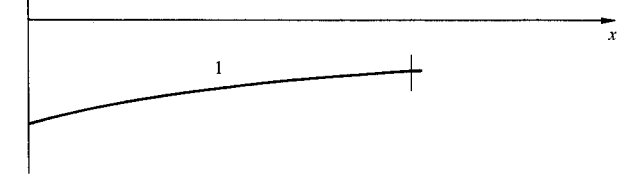


Figure 4 One cycle of drive waveform $V_{\rm a}$ with typical voltage developed across the gas, $V_{\rm g}$, and circuit current i.

Figure 5 Variation of the electric field and related partitioning of the gap.





(c)

Fig. 4. Since $V_{\rm g}$ is represented by the area under the E(x) curve, these two effects tend to drive the field near the anode into the opposite polarity, as indicated in Fig. 5(a). Although the final solution may not have a reversal of field direction within the gap, it is necessary to design the program to handle this possibility for short periods, otherwise the solution "blows up" and computation ceases. When the field is strongly distorted by space charge, electrons moving toward the anode become trapped by the low fields and cannot traverse the entire gap to the anode in time Δt .

• Partition of gap

To take into account the trapping of electrons and reversal of field direction, the gap is partitioned into three regions, as labeled in Fig. 5. Each region is treated differently, depending on its particular characteristics, as detailed below and in the appendixes.

Region 1

For each loop, Δt is calculated such that the ions can just traverse box 1. Region 1 is defined as the boxes which electrons starting at the cathode can traverse in time Δt , driven by the existing E(x); the last box in Region 1 is labeled IJ as shown in Fig. 5. The extent of each region is recalculated each time interval. Since the electron-to-ion mobility ratio is 140, if the field is not greatly distorted, the electrons have time to traverse the entire gap, in which case only Region 1 exists.

Region 2

Also calculated for each time increment is whether, and at which box, the electric field (first) becomes positive. This first box is labeled MA in Fig. 5(a). Region 2 is defined as those boxes bounded by Region 1 and box MA. In this region electrons accumulate but their velocities are relatively low, so that it becomes feasible to track the electrons just as is done for ions. However, the electrons are still moving fast enough to traverse several boxes in Δt . To avoid this, Δt is divided by an integer, NZ, which is computed to just allow electrons to move through the first box of Region 2. The effects of the electron motion are then computed NZ times in each interval Δt .

Region 3

Region 3 is comprised of those boxes between where the field first becomes positive and the anode wall. The same subinterval as for Region 2 is used in Region 3. As shown in Fig. 5(a), the field in Region 3 may first become positive a short distance from the anode.

For all three regions the rate of direct electron-ion recombination in any box is taken to be proportional to the product of the densities of electrons and ions. The change in density of each is, therefore

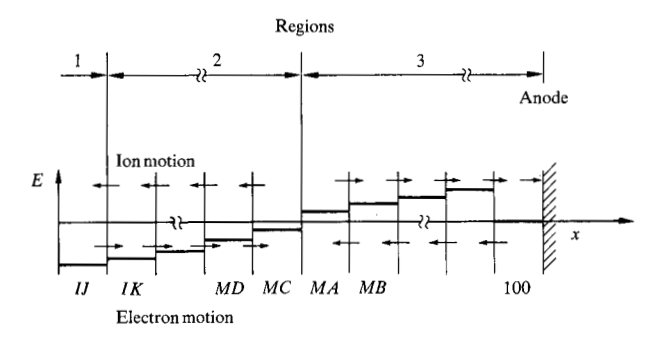


Figure 6 Expanded section of Fig. 5(a) in the neighborhood of the electric field reversal.

$$\Delta p(I) = \Delta n(I) = -Rp(I)n(I)\Delta t, \tag{10}$$

where R has the value of 2.2×10^{-7} cm³ · s⁻¹ [8].

Figure 6 is an expanded view of the box-by-box values of the field, in the neighborhood of its reversal, showing the directions of motion for electrons and ions for various conditions and also the box labels for the regions. Depending on how much space charge has been generated at a particular time, not all three regions need exist.

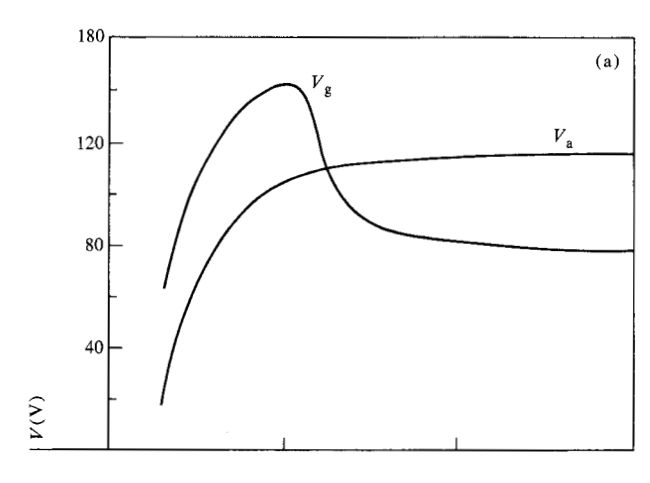
• Computer program

A computer program was developed which has two loops. The main loop consists of a series of detailed operations which are repeated for each of about 2000 time intervals; it is started after the panel parameters and initial conditions are recorded in storage. The recycle loop is used at the end of each firing cycle to reset parameters and establish conditions so that the main loop can be run again for the next firing period. The program converges for drive amplitudes 30 percent above the normal operating range. However, voltages above this value create field gradients which require a finer division of the gap for convergence.

Throughout the description and for the equations used in the appendixes, it is assumed that the right wall is the anode. In practice the anode and cathode reverse roles each half cycle of the applied voltage, and the directions of motion of the charges alternate.

Rather than write a separate program for each halfcycle, it was arranged that the right wall would always be the anode. This is accomplished by reversing the polarity of the charge on the capacitor and transposing the residual charge in the gas space at the end of each firing. In this way the actual problem is simulated by repeatedly solving the same problem but with new initial conditions.

The number of cycles required before the solution reaches stable, cyclic values depends on the accuracy of



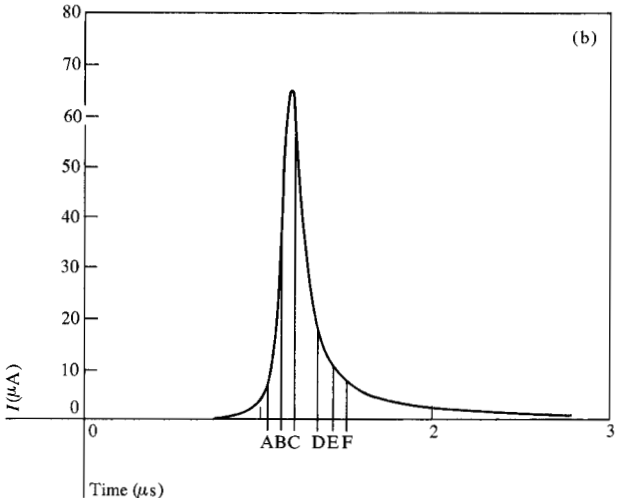


Figure 7 Calculated values of (a) voltage and (b) current across the gap for the first three microseconds of simulated operation. The applied voltage is 114 V. The lines A-F indicates times and currents corresponding to other quantities plotted in Fig. 8.

the initial assumptions for the charge distribution in the gas and the charge condition of the dielectric capacitor. Three or four firings are usually sufficient but the program allows five cycles. The results of the last cycle are automatically plotted by the system.

Results and discussion

The physical parameters of an experimental cell were used in the simulation program so that direct comparison could be made between computed characteristics and experimental data. The input included

Gas: Ne + 0.001 Ar
$$d = 0.125 \text{ mm}$$

 $P = 8 \times 10^4 \text{ Pa}$ $A = 4.7 \times 10^{-2} \text{ mm}^2$
 $\gamma = 0.075$ $C = 0.2 \text{ pF}$

The drive voltage rise-time constant was 0.3 μ s and its amplitude was varied from 100 to 114 V.

237

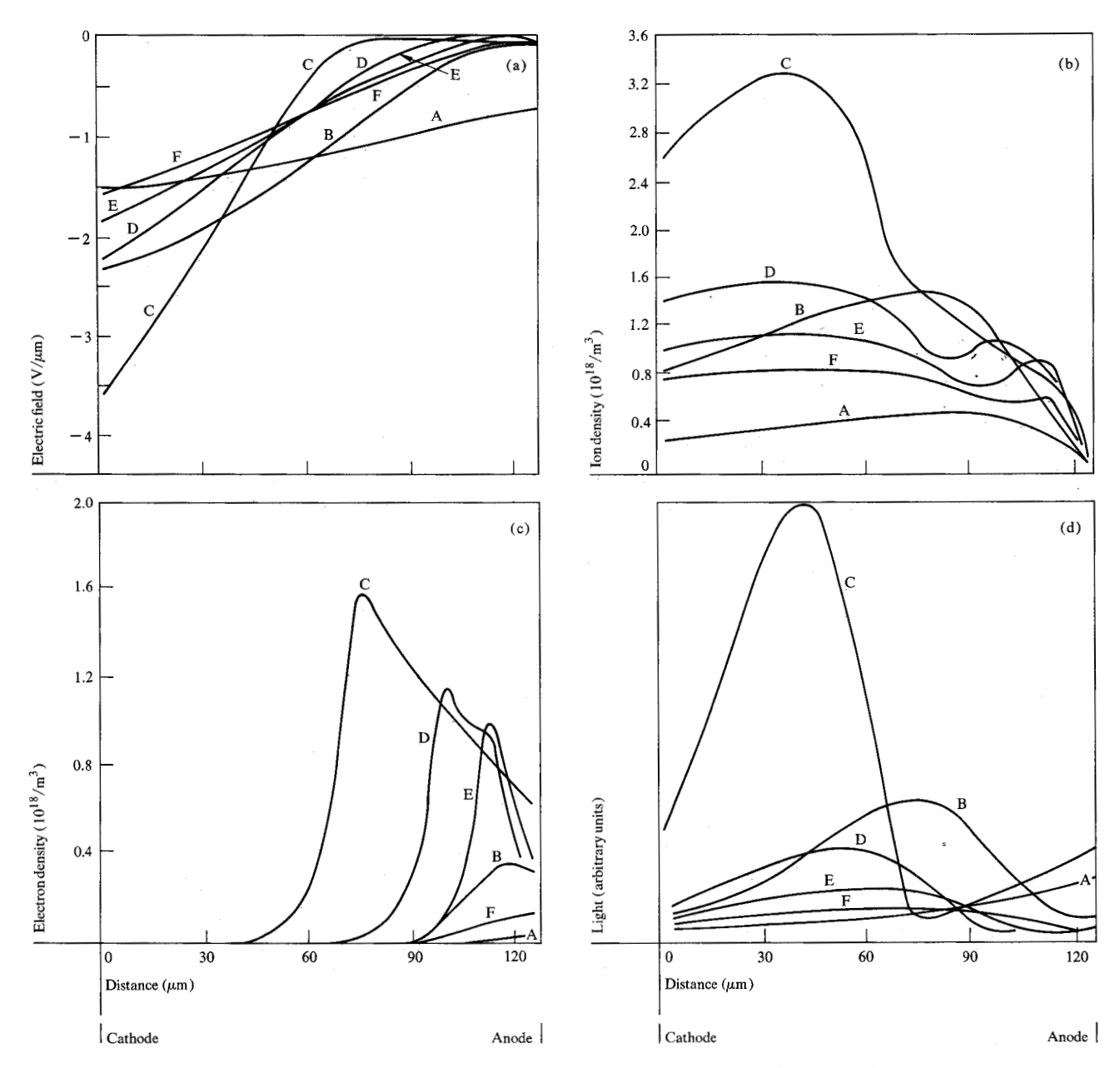


Figure 8 Calculated variation of (a) electric field, (b) ion density, (c) electron density, and (d) relative light output across the gap at the six times indicated in Fig. 7.

Figure 7 is a representative computed plot of the voltage and current across the gas as functions of time for the first 3 μ s of the calculation. Note that a substantial voltage still appears across the gas when the current has virtually decayed to zero. The six marks on the abscissa, labeled A through F, indicate the times for which other quantities are plotted in Fig. 8 by position in the gap.

Figure 8(a) shows six curves of electric field vs distance from the cathode, corresponding to the times indicated in Fig. 7(b). The field at the cathode becomes maximum at about the time the current is maximum.

This may have important consequences when sputtering of the dielectric is considered. The magnitude of this field (36 000 Vcm⁻¹) is about three times the maximum field computed with constant-field models. Near times of maximum current the field is greatly distorted, with only the field near the cathode being nearly linear.

The electric field is very low over a region of about one-third the gap adjacent to the anode. Electrons moving toward the anode become temporarily trapped and are slowly released as the current decays and the fields become more uniform. This slow release of ions and electrons may help explain the long tail at the end of the current pulse. It had previously been assumed that only the slow decay of metastable atoms could account for this current tail.

Figures 8(b) and 8(c) show the densities of ions and electrons vs position for equivalent times. The density of ions at the anode is almost zero since the field sweeps them away as they are generated and none are supplied from the anode wall. The density of electrons is seen to "pile-up" in the low field region as the electrons generated in the high-field region become trapped. The density of electrons may, therefore, momentarily exceed the ion density near the anode, causing the field gradient to become slightly negative.

It was proposed by Vernon and Wang [3] that the rate of generation of excited atoms is probably proportional to the rate of ion generation. Assuming that the excited atoms have very short lifetimes and that a fixed fraction of them produce photons, we can calculate the relative light output as a function of position and time. The average rate of generation of excited atoms (or photons) at any position is proportional to the ion generation rate, $\eta(I) E(I) n(I) v_n(I)$.

Figure 8(d) is a plot of the computed relative light output for the six sample times. The peak of the light output shifts from the anode toward the cathode during times A, B, and C but moves back toward the anode during times, D, E, and F. This behavior is similar to that found experimentally by Anderson [9] using a 2.54-mm (100-mil) gap. The velocity of the light shift from peak B to peak C is found to be 4.4×10^4 cm/s. The motion of the light intensity peak is consistent with Anderson's view of a propagating electric field gradient. The different velocities measured by Anderson $(7 \times 10^5 \text{ cm/s})$ and calculated by Vernon and Wang $(1 \times 10^5 \text{ cm/s})$ may therefore be attributed to their drive voltages of 500 and 175 V, respectively, whereas our result was obtained using 114 V.

Figures 9 and 10 are comparisons of computed and experimental characteristics of the current. The only significant difference between the two appears in Fig. 10(a). Here it was necessary, to avoid the possibility of negative or zero voltage across the gas at the start of a cycle, to start the simulation time at $0.2~\mu s$ instead of zero. Since virtually no current flows during this initial interval, the solution is not affected except for the small delay of the current peak.

Figure 11(a) shows the values of the charge transferred per firing of the cell. The difference of about ten percent between the computed and experimental values can be expected as a consequence of the assumptions made, the accuracy of the published input parameters used, and the general limitations of a one-dimensional model.

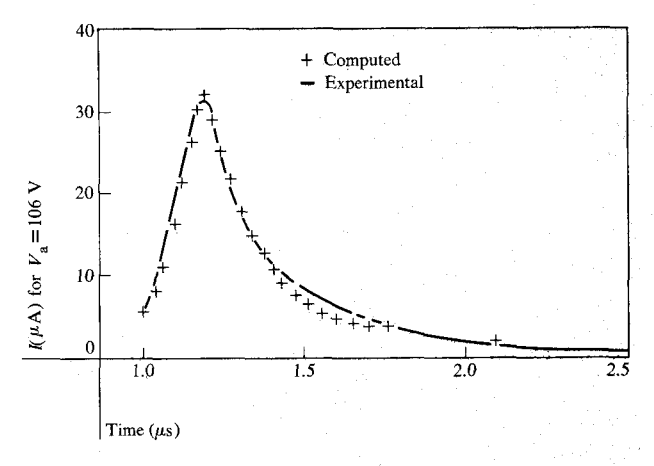
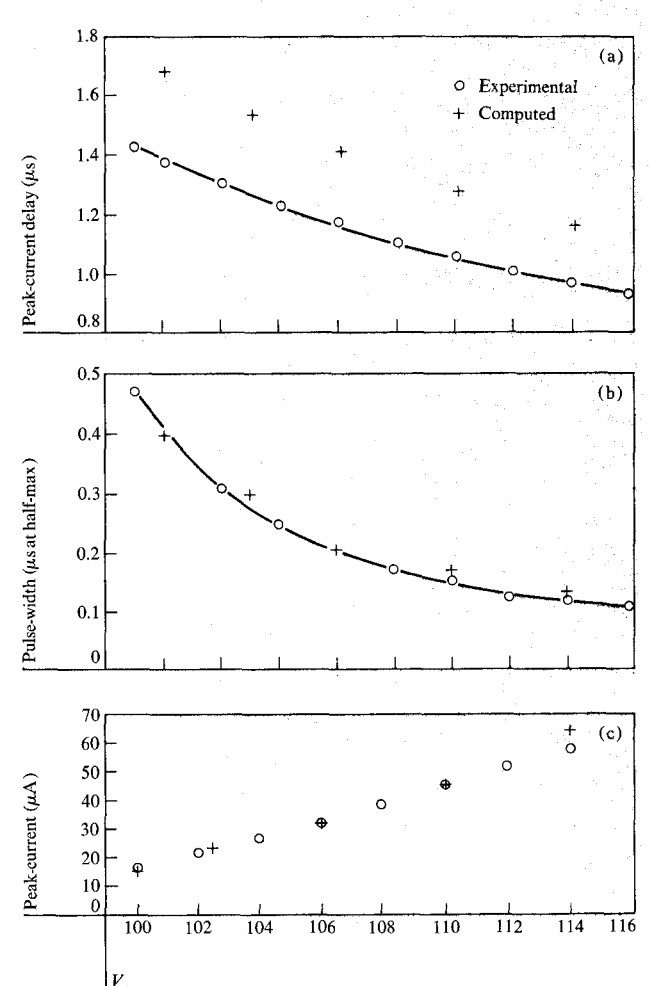
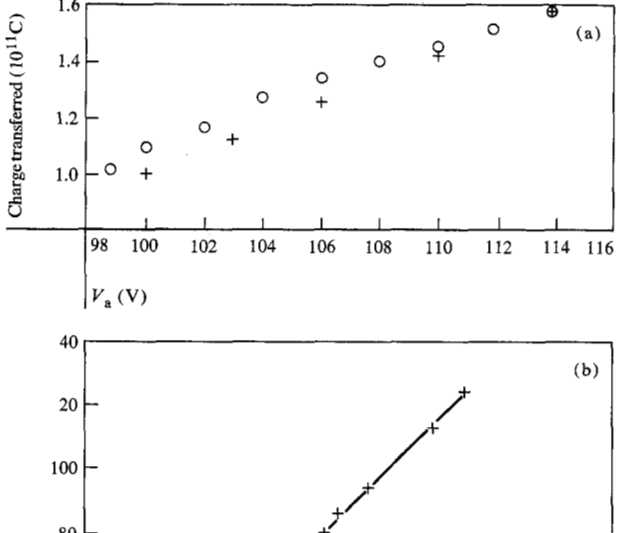


Figure 9 Comparison of simulated and measured circuit current for $V_{\rm a} = 106~V$; solid curve is experimental, cross points are computed.

Figure 10 Characteristics of the external circuit current as functions of applied voltage: (a) delay of the current peak from start of the cycle; (b) duration of the current pulse, measured at half the peak value; and (c) dependence of the peak value on applied voltage. Circles are experimental data, cross points are computed.





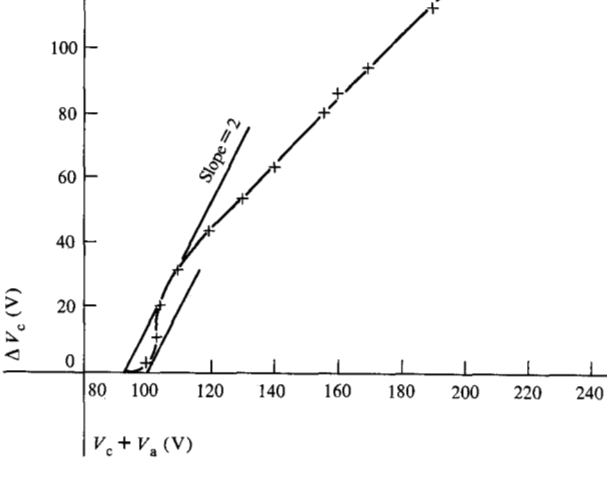


Figure 11 (a) Charge transferred per firing of the cell. (b) Charge-transfer-characteristic curve determined by the method of Refs. 10 and 11.

The concept of a charge-transfer-characteristic curve was first introduced by Slottow and Petty [10, 11]. Straight lines of slope 2, tangent to the curve, intercept the abscissa at the minimum and maximum sustain voltages. Thus, such a curve allows one to determine the stable operating points for a given drive amplitude and the allowable range of sustain voltage for stable cyclic firing.

Figure 11(b) is a plot of the computed charge-transfer-characteristic curve using the panel parameters described previously. The minimum and maximum sustain voltages are 93 and 100 V, respectively, This provides a predicted operating range of 7 V, compared with the 10.5 V measured for the panel after 750 hours of operation.

In view of the approximations made for the model, the results of these calculations are considered to compare well with experiment.

Acknowledgments

Thanks are extended to P. S. Hauge and the late J. F. Woods for their valuable suggestions and detailed discussions concerning the model. I also express my appreciation to M. Klein, F. M. Lay, and B. Welber for their help with evaluations of the various approximations and overall considerations, and to J. J. Hall for use of his experimental data.

References

- F. M. Lay, C. K. Chu and P. H. Haberland, "Simulation of Cyclic Operation of Gas Panel Device," *IBM J. Res. Develop.* 18, 244 (1974); this issue.
- M. Klein, Manufacturing Research Laboratory, IBM Thomas J. Watson Research Center, Yorktown Heights, New York, private communication of results not published.
- H. Vernon and C. C. Wang, "AC Electrical Breakdown of Neon with External Electrodes," J. Appl. Phys. 43, 2664 (1972).
- A. A. Kruithof and F. M. Penning, "Determination of Townsend Ionization Coefficient α for Mixtures of Neon and Argon," *Physica (Utr.)* 4, 430 (1937).
 F. M. Lay, "Relative Photoelectric Emission of Some Metal
- F. M. Lay, "Relative Photoelectric Emission of Some Metal Films and Dielectrics in a Glow Discharge," TR 21.420, IBM Systems Development Division Laboratory, Kingston, New York, March 1971.
- M. A. Biondi and L. M. Chanin, "Mobilities of Atomic and Molecular Ions in the Noble Gases, *Phys. Rev.* 94, 910 (1954).
- J. M. Anderson, "Hall Effect and Electron Drift Velocities in the Plasma of the Positive Column," Phys. Fluids 7, 1517 (1964).
- H. J. Oskam and V. R. Mittelstadt, "Ion Mobilities in Helium, Neon and Argon," Phys. Rev. 132, 1435 (1963).
- J. M. Anderson, "Electrodeless Discharge Modes in Neon-Nitrogen Mixture with Application to the Plasma Display Panel," Appl. Phys. Letters 16, 531 (1970).
- H. G. Slottow and W. D. Petty, "Stability of Discharge Series in the Plasma Display Panel," *IEEE Trans. Electron Devices* ED-18, 650 (1971).
- W. D. Petty and H. G. Slottow, "Critical Voltage Parameters in Addressing the Plasma Display Panel," presented at IEEE Device Meeting, Washington, D.C., October 13, 1971.

Appendix A: Ion density changes due to ion motion

• Regions 1 and 2

In these regions the electric field is negative and the ions move toward the cathode. The ion density of the *I*th box is increased by an inflow of ions from the (I + 1)th box and decreased by the flow of ions out of the *I*th box and into the (I - 1)th box during the particular time interval Δt .

The change in ion density is according to Eq. (3)

$$\Delta p(I) = \Delta t [p(I+1)v_{\rm p}(I+1) - p(I)v_{\rm p}(I)]/\Delta x.$$
 (A1)

In the event that I=1, the ions flowing out are neutralized at the cathode wall and in the process produce the secondary electrons. For the special case when I=100, ions leave to enter box 99, but no ions enter from the

anode wall. In this way the anode boundary condition is satisfied. Equation (A1) applies to boxes 1 through 99. For box 100, the following equation is used:

$$\Delta p(100) = -p(100)v_{\rm p}(100) \Delta t/\Delta x.$$
 (A2)

• Region 3

When a Region 3 exists, the electric field in this region is positive and the ions move toward the anode. For reasons similar to those for Regions 1 and 2, the change in ion density of the *I*th box is

$$\Delta p(I) = \Delta t \left[p(I-1)v_{\rm p}(I-1) - p(I)v_{\rm p}(I) \right] / \Delta x. \quad (A3)$$

In this region Eq. (A3) applies also to box 100 since ions can flow out of this box and become neutralized at the anode wall. However, the first box (labeled MA in Fig. 6) is a special case since no ions can flow into this box due to the reversal of electric field. Fox box MA then.

$$\Delta p(MA) = -\Delta t \ p(MA) \ v_{p}(MA) / \Delta x. \tag{A4}$$

Appendix B: Number and density of electrons

• Region I

By definition, Region 1 consists of those boxes which the electrons pass through completely during time Δt . This implies that there is no accumulation of electrons from previous intervals. Rather than attempt to keep track of the electrons as is done for ions, an average electron density is deduced. To do so, it is first necessary to compute the number of electrons that pass the right edge of each box.

For any time interval Δt , the number of secondary electrons that leave a unit area of the cathode is γ times the number of ions that arrive at the cathode during that interval, or

$$N_{\rm c} = \gamma \, p(1) \, v_{\rm p}(1) \, \Delta t. \tag{B1}$$

In the process of passing through the first box the number of electrons grows exponentially [Eq. (1)] so that

$$N(1) = N_c \exp[\eta(1)|E(1)|\Delta x].$$
 (B2)

In a similar way N(1) "exponentiates" through box 2 so that the number of electrons at each box can be calculated sequentially with

$$N(I) = N(I-1) \exp[\eta(I) | E(I) | \Delta x].$$
 (B3]

where I takes on values of 2 to IJ (see Fig. 6). Since the electrons move through each box in a time short compared to Δt , the average electron density in any box is taken to be

$$\bar{n}(I) = N(I) / v_{n}(I) \Delta t. \tag{B4}$$

This methed of determining the density of electrons in Region 1 assumes that a number $N_{\rm c}$ of electrons leave the cathode in a group during each Δt . The results are the same if one considers the electrons to be generated at a continuous rate and the electron density is determined by dividing the generation rate by the electron velocity at the cathode.

• Region 2

In Region 2 the electric field is negative but relatively small in amplitude. The electrons move toward the anode with a correspondingly low velocity so that those which arrive during the current Δt accumulate with those which are still present from previous time intervals. In this region it is necessary to keep track of the electrons as they move and exponentiate through the gas exactly as done for the ions. This is feasible since the electron velocities are low and a reasonable size time interval can be used. However, Δt is still too large and would allow the electrons to move through many boxes. To prevent this, Δt is divided by an integer factor NZ, whose value is computed each loop, such that the electrons just traverse the first box of Region 2. Since the magnitude of the field is decreasing in the direction of the anode, the electrons in other boxes of this region move a distance less than Δx . For each subinterval, the density of electrons in each box of Region 2 is updated; however, for each main loop the subinterval calculations are repeated NZ times. This description applies when there is no Region 3.

If a Region 3 also exists, a similar procedure is followed except that Δt is divided by ten and each subinterval calculation is repeated ten times. In this case, however, at the end of each subinterval Poisson's equation is imposed to slightly modify the fields, and therefore the electron velocities, in Regions 2 and 3.

The density of electrons in any box changes for two reasons. 1) The inflow and outflow rates in any box are unequal due to the variations of field and velocity with position and 2) as the electrons enter a box they also increase in number due to the avalanche process. This leads to the following expression for the change in electron density for one subinterval when Region 3 does not exist:

$$\Delta n(I) = \{ n(I-1)v_{n}(I-1)$$

$$\times \exp[\eta(I)|E(I)|v_{n}(I)|(\Delta t/NZ)]$$

$$- n(I)v_{n}(I) \} (\Delta t/NZ\Delta x).$$
(B5)

When Region 3 does exist, the same expression is used with NZ = 10. Equation (B5) applies for boxes IK through MC (see Fig. 6). However, the last box (MC) in Region 2 requires special treatment when Region 3

241

exists since electrons can enter but not leave due to the field reversal. In this case,

$$\Delta n(MC) = \{n(MD)v_{n}(MD) (\Delta t/10)$$

$$\times \exp[\eta(MC)|E|(MC)v_{n}(MC)$$

$$\times (\Delta t/10)]\}/\Delta x.$$
(B6)

• Region 3

Although it is not fully indicated in Fig. 6, when Region 3 exists the electric fields become slightly positive, but it is also possible for the fields to become slightly negative again near the anode. It is therefore necessary to test each box for the polarity of the field before one can determine the change in electron density. Since the magnitude of the electric field is small in the vicinity of a polarity reversal, we assume that η is so small that no ionizing collision occurs. The change in electron density is due only to the difference between in- and out-flow of electrons.

In addition to testing for field polarity it is also necessary to make two other tests.

- 1. Does the first box of Region 3 happen to be box 100? If it is, the electrons are trapped in this box since none can exit due to the field reversal and none can enter from the anode wall.
- 2. Is MB = 100? If so, electrons can only exit the box and none enter from the anode wall. This condition also prevails for box 100 if neither MA nor MB = 100, and if the field is positive. If the field is negative, electrons can both enter and leave box 100.

Aside from these special cases, the following equations apply for each subinterval:

Positive field

$$\Delta n(I) = [-n(I+1)v_{\rm n}(I+1)(\Delta t/10) + n(I)v_{\rm n}(I)(\Delta t/10)]/\Delta x$$
(B7)

for I = MB to 99, and

$$\Delta n(100) = [n(100)v_{\rm n}(100)(\Delta t/10)]/\Delta x.$$
 (B8)

The signs in these two equations reflect the fact that when the field is positive, the electron velocities are negative.

Negative field

$$\Delta n(I) = \left[n(I-1)v_{\rm n}(I-1) - n(I)v_{\rm n}(I) \right] (\Delta t / 10\Delta x). \tag{B9}$$

for I = MB to 100.

The number of electrons in any box of Region 2 or 3 is given by

$$N(I) = n(I) \Delta x. \tag{B10}$$

Appendix C: Ion density changes due to ionizing collisions

• Region 1

Equations (B2) and (B3) of Appendix B give the number of electrons at the right-hand edge of any box during an avalanche process. Since in this region there are no residual electrons from the previous interval, and since the avalanche process produces electron-ion pairs, the change in ion density due to this mechanism is

$$\Delta p(I) = \lceil N(I) - N(I-1) \rceil / \Delta x. \tag{C1}$$

• Region 2

The increase in the density of ions for each subinterval in this region depends on the current collision process. If N_1 electrons enter box I and exponentiate, the number of ions generated would be $N_1\{\exp[\eta(I)V(I)]-1\}$ or, using the first two terms of a series expansion, $N_1\eta(I)V(I)$. The number of electrons that enter box I is $n(I-1)v_n(I-1)\Delta t/NZ$, so that the change in ion density is

$$\Delta p(I) = [n(I-1)v_{n}(I-1)\eta(I)|E(I)|v_{n}(I)](\Delta t/NZ)^{2}(\Delta x)^{-1}.$$
(C2)

• Region 3

Consistent with the assumption made in Appendix B for Region 3, namely, that the magnitude of the electric field is so low that virtually no ionization occurs, it is assumed that $\Delta p(I) = 0$.

Appendix D: Current and charge flow in the external circuit

In a one-dimensional situation, when a quantity of charge, Q, moves with a velocity v between two electrodes separated by a distance d, the instantaneous current that flows in the external circuit is i = Qv/d, which implicitly includes displacement current.

If the charge Q moves through a fraction of d, say x, the amount of charge, Q_1 , which crosses any cross section of the external circuit is

$$Q_1 = Qx/d. (D1)$$

The total ion component of current is the sum of the contributions from all boxes. The total charge flow due to ions during any time interval is

$$Q_{\rm p} = i_{\rm p} \Delta t. \tag{D2}$$

Since the electron current component may not flow during the entire time interval Δt , Eq. (D1) is first applied sequentially to each box, to determine the charge flow

due to electrons. The average electron current component is then determined by

$$\bar{i}_{\rm p} = Q_{\rm p}/\Delta t. \tag{D3}$$

The total current and charge transfer are the sums of the two components,

$$i = i_n + \overline{i}_n$$
 and $Q = Q_p + Q_n$. (D4)

Application of these equations to each box automatically takes into account the fact that charge is generated within the gap and that, therefore, all the charged particles do not move the same distance to arrive at the anode or cathode.

• Ion component-all regions

$$i_{\rm p} = (Aq\Delta x/d) \sum_{1}^{100} p(I)v_{\rm p}(I).$$
 (D5)

Since the sign of v_p changes when the field reverses, Eq. (D5) can be applied directly to all three regions.

• Electron component

Region 1 Equations (B2) and (B3) describe the number of electrons in any box of Region 1. The charge which

flows in the external circuit due to motion of electrons in any box is

$$Q_{n}(I) = AqN(I) \Delta x/d.$$
 (D6)

The total charge transfer due to Region 1 is the sum of the effects of all boxes in that region.

Regions 2 and 3 In these regions the electrons do not move through an entire box during each subinterval, so an average number of electrons in each box is used. The charge flow due to any one box for each subinterval is them

$$Q_{n}(I) = \frac{1}{2}(Aq/d)[N(I) + N(I-1)]v_{n}(I)\Delta t/NZ.$$
 (D7)

The sign of the velocity term takes into account the field reversals. By summing the $Q_{\rm n}(I)$ for the subintervals and, successively, the $Q_{\rm n}$ for the boxes and regions, the total $Q_{\rm n}$ is obtained. This total is used in Eq. (D3) to determine the average electron current component for that time interval.

Received December 3, 1973

The author is located at the IBM Thomas J. Watson Research Center, Yorktown Heights, New York 10598.